Journal of Catalysis **189,** 147–157 (2000)
Article ID jcat.1999.2689, available online at http://www.idealibrary.com on IDEAL®

Selective Oxidation of *n*-Butane and Butenes over Vanadium-Containing Catalysts

J. M. López Nieto,*,[1] P. Concepción,†,[2] A. Dejoz,‡ H. Knözinger,† F. Melo,* and M. I. Vázquez‡

*Instituto de Tecnología Química, UPV-CSIC, Avenida de los Naranjos s/n, 46022 Valencia, Spain; †Institut für Physikalische Chemie, University of München, Bütenandtstrasse 5-13, Haus E, 81377 München, Germany; and ‡Departamento de Ingeniería Química, Universidad de Valencia, Dr. Moliner 50, 46100 Burjassot, Spain

Received June 14, 1999; revised September 7, 1999; accepted September 20, 1999

The oxidative dehydrogenation (OXDH) of *n*-butane, 1-butene, and *trans*-2-butene on different vanadia catalysts has been compared. MgO, alumina, and Mg–Al mixed oxides with Mg/(Al + Mg) ratios of 0.25 and 0.75 were used as supports. The catalytic data indicate that the higher the acid character of catalysts the lower is both the selectivity to C_4-olefins from *n*-butane and the selectivity to butadiene from both 1-butene or *trans*-2-butene. Thus, OXDH reactions are mainly observed from *n*-butane and butenes on basic catalysts. The different catalytic performance of both types of catalysts is a consequence of the isomerization of olefins on acid sites, which appears to be a competitive reaction with the selective way, i.e., the oxydehydrogenation process by a redox mechanism. Infrared spectroscopy data of 1-butene adsorbed on supported vanadium oxide catalysts suggest the presence of different adsorbed species. O-containing species (carbonyl and alkoxide species) are observed on catalysts with acid sites while adsorbed butadiene species are observed on catalysts with basic sites. According to these results a reaction network for the oxydehydrogenation of *n*-butane is proposed with parallel and consecutive reactions.

Key Words: **oxydehydrogenation (*n*-butane, butenes) on supported vanadia (vanadium oxide, vanadate) catalysts; alkane oxidation; catalyst characterization; infrared spectra of 1-butene adsorbed; ^{51}V NMR; diffuse reflectance.**

INTRODUCTION

Supported vanadia catalysts are among of the most important solid catalysts for the selective oxidation of short chain alkanes (1–6), i.e., selective O- or N-insertion or oxidative dehydrogenation (OXDH) reactions. However, their catalytic behavior depends on the V-loading and the nature of the metal oxide support.

In the case of OXDH reactions V–Mg–O mixed metal oxides (6–11) and VO_x/Al_2O_3 have been the most studied catalysts (12–15). In both cases, VO_4 tetrahedra appear to be the selective sites. Therefore, one might expect that both catalysts could be used in selective OXDH reactions. However, it is known that their catalytic behavior strongly depends on the alkane feed (13, 16, 17). Thus, V–Mg–O mixed metal oxides are the most selective catalysts in the OXDH of butane to butenes and butadiene, while VO_x/Al_2O_3 catalysts have been reported as the most active and selective catalysts for the OXDH of ethane (12–15). It has thus been suggested that the second H abstraction and/or the desorption of olefinic intermediates may be the selectivity determining steps which are expected to depend on the acid–base character of the catalysts (17). The presence of acid–base sites on selective catalysts should influence the interaction between the olefinic intermediates and the catalysts, thus affecting the selectivity to OXDH products.

During the oxidation of *n*-butane on supported vanadium oxide catalysts, isomerization of olefins, in addition to oxydehydrogenation and deep oxidation, can be observed. Since isomerization of olefins is favored by the presence of acid sites, OXDH of *n*-butane and butenes could be used as test reactions to study the influence of the presence of acid and/or basic sites on the oxidation of *n*-butane and the distribution of oxydehydrogenation products, i.e., mono- and diolefins.

The aim of the present work is to investigate the catalytic behavior of supported vanadium oxide catalysts during the oxidation of *n*-butane and butenes, using metal oxide supports with different acid–base character. Well-characterized and selective catalysts, in which tetrahedral V species are exclusively present in the catalysts have been employed. In addition, an *in situ* IR-spectroscopy study of adsorption of 1-butene on supported vanadia catalysts has been carried out in order to characterize the nature of adsorbed species formed on the catalysts during the reaction. According to these results, a reaction network with parallel and consecutive reactions is proposed.

[1] To whom correspondence should be addressed. Fax: 34-96-3877809. E-mail: jmlopez@itq.upv.es.
[2] On leave from the Instituto de Tecnología Química, Valencia, Spain.

0021-9715/00 $35.00

EXPERIMENTAL

Catalyst Preparation

Commercial γ-Al_2O_3 (Girdler T126), synthesized MgO, and heat-treated Mg–Al mixed oxides with hydrotalcite and spinel structures have been employed as support and are referred to as Al_2O_3, MgO, HT, and ESP, respectively. MgO was obtained from magnesium oxalate by calcination in air at 700°C for 3 h (17). Mg–Al–O mixed oxides with hydrotalcite and spinel structures were obtained by continuous coprecipitation of aqueous solutions of magnesium and aluminum nitrates with theoretical Al/Mg atomic ratios of 0.33 and 3.0, respectively, at a constant pH of 13 and at room temperature (17). In both cases the gel obtained was aged at 60°C for 18 h and then filtered and washed until a pH of 7 was obtained. The solids were then dried at 100°C overnight and calcined in air at 450°C for 18 h.

Supported vanadium catalysts were prepared by impregnation of the metal oxide supports with ammonium metavanadate aqueous solutions, according to the preparation procedure reported previously (15, 17). Then, the solids were filtered and dried at 80°C for 16 h. In all cases, the samples were calcined at 600°C for 4 h.

Catalyst Characterization

Infrared spectra of adsorbed pyridine were obtained in a Nicolet 710 FTIR spectrophotometer. Wafers of 10 mg cm^{-2} were mounted in a pyrex vacuum cell fitted with CaF_2 windows. The samples were degassed at 400°C for 2 h and then cooled at room temperature to obtain the original IR spectra. Then, pyridine was admitted at room temperature, degassed for 1 h in order to remove the physisorbed fraction, and the spectra were taken at room temperature. Finally, pyridine was desorbed at temperatures of 150 and 250°C.

IR spectroscopy studies of 1-butene adsorption were carried out on a Bruker IFS-88 apparatus at a spectral resolution of 1 cm^{-1} and collecting 128 scans. Self-supporting wafers were prepared from the sample powders and heated directly in the IR cell. Prior to each experiment all the samples were activated for 1 h in a flow of oxygen at 500°C, followed by 1 h evacuation at the same temperature. The experiments were performed by introducing 50 hPa (1 hPa = 1 mbar) of 1-butene at room temperature into the IR cell. After 1 h the temperature was increased from 25 to 450°C by steps of 50°C and stabilization times of 1 h at each temperature.

Temperature-programmed reduction (TPR) results were obtained in a Micromeritics apparatus loaded with 100 mg of catalyst. The samples were first treated in argon at room temperature for 1 h. The samples were subsequently contacted with an H_2/Ar mixture (H_2/Ar molar ratio of 0.15 and a total flow of 50 ml min^{-1}) and heated, at a rate of 10°C min^{-1}, to a final temperature of 1000°C.

Catalytic Tests

The catalytic experiments were carried out in a fixed bed quartz tubular reactor (i.d. 20 mm, length 400 mm) working at atmospheric pressure. The reactor was equipped with a coaxial thermocouple for catalytic bed temperature profiling. Catalyst samples (0.3–0.5 mm particle size) were introduced in the reactor and diluted with 8 g of silicon carbide (0.5–0.75 mm particle size) in order to keep a constant volume in the catalyst bed. The flow rate of the reactants was varied (100–600 cm^3 min^{-1}) to achieve different contact times ($W/F = 2$–$40\ g_{cat}\ h\ mol_{C_4}^{-1}$) and different *n*-butane conversion levels. The feed consisted of mixtures of *n*-butane/oxygen/helium or butenes/oxygen/helium with molar ratios of 5/20/75 or 2/20/78, respectively. Experiments were carried out in the 400–550°C temperature interval. Reactants and reaction products were analyzed by on-line gas chromatography, using a Hewlett-Packard apparatus equipped with two columns in parallel: (i) 23% SP-1700 Chromosorb PAW (30 × 1/8 in.) to separate hydrocarbons and CO_2; (ii) Carbosieve-S_o (8 × 1/8 in.) to separate O_2 and CO. Blank runs showed that under the experimental conditions used in this work the homogeneous reaction could be neglected.

RESULTS AND DISCUSSION

Catalyst Characterization

The characterization data of the various catalysts are compared in Table 1. TPR patterns indicate that the reducibility of V^{5+} species decreases in the following sequence: $VO_x/Al_2O_3 > VO_x/ESP > VMgO > VO_x/HT$. On the other hand, the amount of Lewis acid sites on the catalysts, determined from the IR spectra of adsorbed pyridine after an evacuation at 150°C, are similar to those observed on pure supports: $Al_2O_3 > ESP > HT > MgO$ (17).

^{51}V NMR and DR–UV–vis spectra showed V^{5+} species with a tetrahedral environment although the aggregation degree of these species depends on the acid nature of the support (17, 22). Thus, the higher the acid character of the support the higher is the aggregation degree of vanadium species.

IR Study of 1-Butene Adsorption

Figure 1 shows the spectra recorded during the adsorption of 1-butene at room temperature on VO_x/Al_2O_3 and their evolution at increasing temperatures. The room temperature spectrum is characterized by the presence of several bands and shoulders at 1692, 1667, 1643, 1600 (broad), 1463 (vw), 1378, and 1181 cm^{-1} (Fig. 1, spectrum b). The sharp band at 1643 cm^{-1} is due to adsorbed unreacted 1-butene (ν (C=C)). In the OH region (not shown) of the VO_x/Al_2O_3 sample outgassed at 500°C three bands are observed at 3740, 3677, and a broad one at 3577 cm^{-1}. The

TABLE 1

Characterization Results of Supported Vanadium Oxide Catalysts

Catalyst	V content (V_2O_5 wt%)	S_{BET} ($m^2\ g^{-1}$)	TPR (°C)[a]		Relative acidity[b]	Type of V species[c]	Rate constant ($mol_{C4}\ h^{-1}\ g_{cat}^{-1}$)[d]	
			T_i	T_{max}			*n*-Butane	1-Butene
VO_x/Al_2O_3	3.5	160	300	465	1.0	$(VO_3)_n$	2.80	2.95[e]
VO_x/ESP	20.0	210	400	540	0.6	$(VO_3)_n$, VO_4	0.78	3.69
VO_x/HT	37.3	166	421	585	0.2	VO_4[f]	0.50	2.02
VMgO	20.1	108	450	568	0.1	VO_4	0.78	2.37

[a] TPR results; T_i, initial reduction temperature; T_{max}, temperature of the maximum hydrogen consumption.

[b] The number of acid sites was determined from the intensity of the corresponding band in the IR spectrum of pyridine adsorbed after desorption at 150°C. Lewis acid sites (band at 1450 cm^{-1}) were only observed.

[c] Determined by ^{51}V NMR and diffuse reflectance (UV–vis).

[d] Rate constant of the oxidation of *n*-butane and 1-butene, supposing pseudo-first-order, at a reaction temperature of 500°C.

[e] Rate constant of the oxidation of 1-butene, supposing pseudo-first-order, at a reaction temperature of 400°C.

[f] With the presence of $Mg_2V_2O_7$ species.

bands at 3740 and 3677 cm^{-1} are perturbed after interaction with 1-butene at room temperature, indicating that olefins interact with the OH groups by π-bonding. The broad feature near 1600 cm^{-1} is referred to the corresponding –C=C– streching mode. In addition to these molecularly adsorbed species, which are easily eliminated by evacuation, other species are also detected. The bands at 1692, 1463, 1378, and 1181 cm^{-1} can be attributed to adsorbed methyl ethyl ketone (C=O stretching, asymmetric and symmetric CH_3 bendings, and C–C–C asymmetric stretching, respectively). While bands at 1667, 1634, and 1173 cm^{-1} can be assigned to methyl vinyl ketone (23). The formation of the methyl vinyl ketone may involve an alkoxide intermediate, which is subsequently oxidized to the corresponding carbonyl compounds. However, no bands in the 1100 cm^{-1} region are detected, indicating the absence of

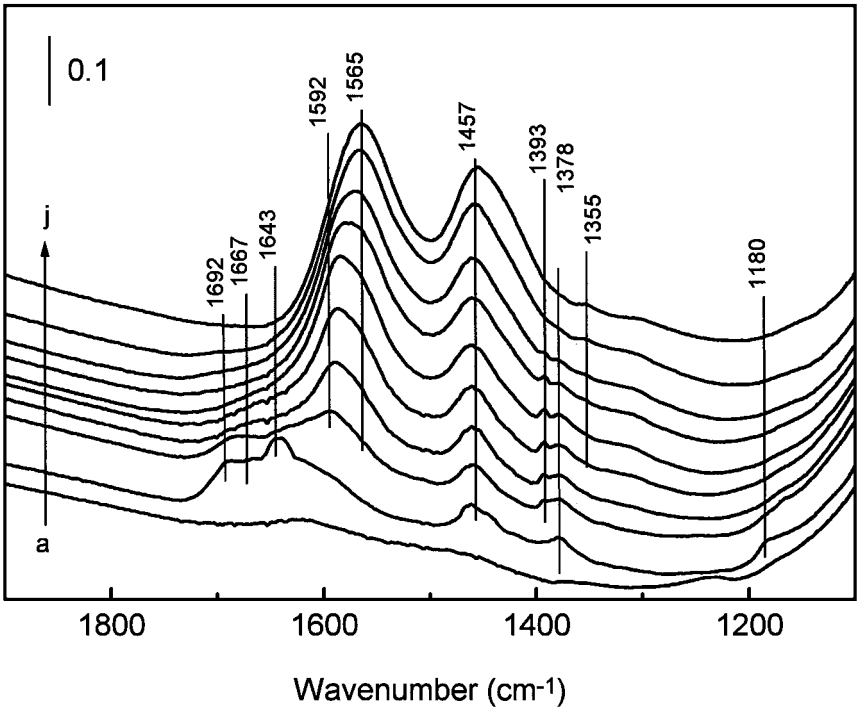

FIG. 1. FT-IR spectra of the VO_x/Al_2O_3 catalyst outgassed at 500°C (a) and after adsorption of 1-butene at increasing temperatures: 25°C, 20 min (b); 100°C, 10 min (c); 150°C, 15 min (d); 200°C, 10 min (e); 250°C, 10 min (f); 300°C, 5 min (g); 300°C, 30 min (h); 350°C, 30 min (i); and 450°C, 40 min (j).

C–O bonds, and therefore of alkoxide species. This might be due to a quick oxidation of the alkoxide species to the corresponding carbonyl compound.

After heating at 100°C, the sharp band at 1643 cm^{-1} due to unreacted 1-butene disappears, whereas new bands at 1592 and 1393 cm^{-1} appear (Fig. 1, spectrum c). These bands might be assigned to species containing carboxylate groups (COO^- asymmetric and symmetric stretching modes) (23). However, the symmetric stretching of COO^- normally appears at higher frequencies (1480–1420 cm^{-1}). On the other hand, the band at 1592 cm^{-1} can also be assigned as a C=C stretching mode, shifted to lower frequencies with respect to the value of the free olefin due to perturbation by adsorption interactions (24). In this sense, surface σ-bonded allyl species can be proposed. These species can be formed by hydrogen abstraction from the allylic position of 1-butene probably by vanadium ions. Expected vinylic C–H modes above 3000 cm^{-1} could not be observed. On the other hand, π-bonded allyl species have been reported in the literature to give characteristic bands at 1468 and 1165 cm^{-1} due to the asymmetric and symmetric C–C–C stretching modes (25). However, a band at 1611 cm^{-1} has been attributed to a surface π-complex of 1-butene adsorbed on Mo(VI)/SiO_2 samples (26). Similar bands have been reported by Kokes *et al.* (27, 28) to π-complexes of adsorbed butenes on ZnO. Also π-complexes of butenes have been observed on silica, Na–Y zeolites and TiO_2 during low-temperature studies by Busca *et al.* (29). According to these results, the band observed at 1592 cm^{-1} can also be assigned to an allylic π-bonded intermediate. Further heating causes the progressive disappearance of the bands at 1690 and 1667 (carbonyl compounds) and the appearance of strong and broad bands at 1565 and 1457 cm^{-1}. These bands are attributed to species containing carboxylate groups. Also in the OH region stretching a broad band around 3650 cm^{-1} confirms the presence of carboxylate species. At temperature above 300°C a new band at 1355 cm^{-1} (vw), assigned to acetate species (23), appears, while the bands at 1592, 1393, and 1378 cm^{-1} tend to disappear. Knözinger *et al.* (30) proposed the formation of carboxylic species from ketones on Al_2O_3 catalysts by a nucleophilic attack of a reactive OH^- group at the carbonyl carbon of a coordinated ketone molecule. In the present case, the formation of carboxylate species can be attributed to a high reactivity of the vanadium species and a strong interaction of the ketone with the surface. At temperatures above 300°C, a broad band near 3050 cm^{-1} starts to appear. This band together with a band at 1600 cm^{-1} (which in our case is superimposed by the broad band centered at 1565 cm^{-1}), has been attributed to unsaturated and/or aromatic compounds, indicating that strongly bonded carbonaceous species began to grow on the surface at higher temperatures (31).

The spectrum resulting from adsorption of 1-butene at room temperature on the VMgO catalyst shows bands at 1673, 1634, 1400, and 1221 cm^{-1} (Fig. 2). The sharp band at 1634 is slightly shifted to lower frequencies relative to

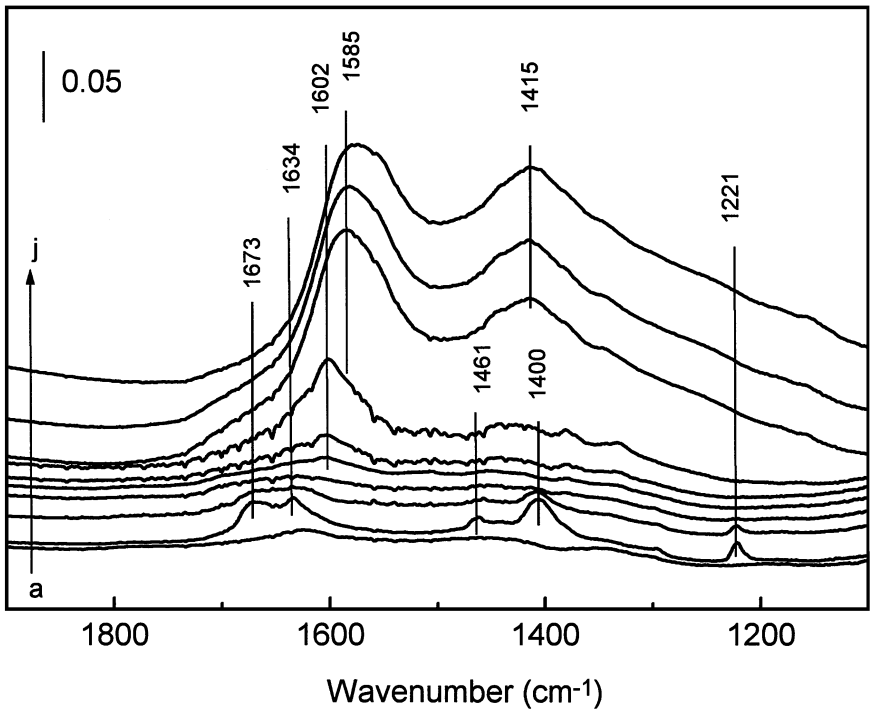

FIG. 2. FT-IR spectra of the VMgO catalyst outgassed at 500°C (a) and after adsorption of 1-butene at increasing temperatures: 25°C, 30 min (b); 100°C, 20 min (c); 150°C, 20 min (d); 200°C, 5 min (e); 200°C, 15 min (f); 250°C, 20 min (g); 350°C, 5 min (h); 350°C, 30 min (i); and 450°C, 30 min (j).

the gas phase (ν (C=C)) double bond stretching mode at 1648 cm^{-1} and can be assigned to unreacted adsorbed 1-butene.

In the OH region of the VMgO sample outgassed at 500°C two bands, at 3722 cm^{-1} (due to Mg–OH species) and a very small band at 3675 cm^{-1} (due to V–OH), are observed. No perturbations of these bands were observed after introduction of 1-butene at room temperature. However, a new band around 3625 cm^{-1} appeared. This band together with the bands at 1673 and 1221 cm^{-1} are characteristic of bicarbonate species (32). Other authors assigned two sharp and very intense bands around 1682–1665 and 1245 cm^{-1} as the C=O stretching frequency and the antisymmetric C–C–C stretching mode of adsorbed acetone species (33). In both cases, the formation of these species can be tentatively explained by a complete or partial degradation of the adsorbed 1-butene molecule due to reactive nucleophilic groups present on the free MgO support. Increasing the temperature to 150°C causes the sudden disappearance of all these bands, indicating a weak interaction and/or low stability of the above species with the surface (Fig. 2, spectrum d). It is interesting to note that no carbonyls or alkoxide intermediate species (as on the VO_x/Al_2O_3 catalysts) are observed. Further heating up to 250°C causes the appearance of a very broad and intense band centered at 1602 cm^{-1}. Other weak broad bands with maximum at 1508, 1448, 1380, and 1331 cm^{-1} are also observed (Fig. 2, spectrum g). No band at 3050 cm^{-1} was detected, indicating that the band around 1600 cm^{-1} is not due to the formation of unsaturated carbonaceous deposits on the catalyst. However, this spectrum is consistent with that of adsorbed butadiene species (34). At temperatures above 300°C the predominant features are those of adsorbed carboxylate and acetate species (very broad and intense bands at 1585 and 1445–1416 cm^{-1}). A broad band at 3050 cm^{-1} due to carbonaceous deposits on the surface is also observed at the highest temperatures. The absence of any intermediate species adsorbed on the catalyst at low temperature seems to indicate a rapid reaction and desorption of the intermediate species. Butadiene, formed by OXDH (see below), due to its higher reactivity, is readsorbed at higher temperatures from the gas phase on the surface of the VMgO catalysts and undergoes further oxidation to carboxylate species.

Figure 3 presents the spectra of the adsorbed species resulting from adsorption of 1-butene at room temperature on VO_x/ESP catalyst and their evolution at increasing temperatures. In addition to bands at 1464, 1438, and 1380 cm^{-1}, the spectrum recorded at room temperature exhibits a sharp ν(C=C) band at 1628 cm^{-1} due to adsorbed unreacted 1-butene. These species are quickly removed by increasing the temperature up to 100°C. At 150°C a new

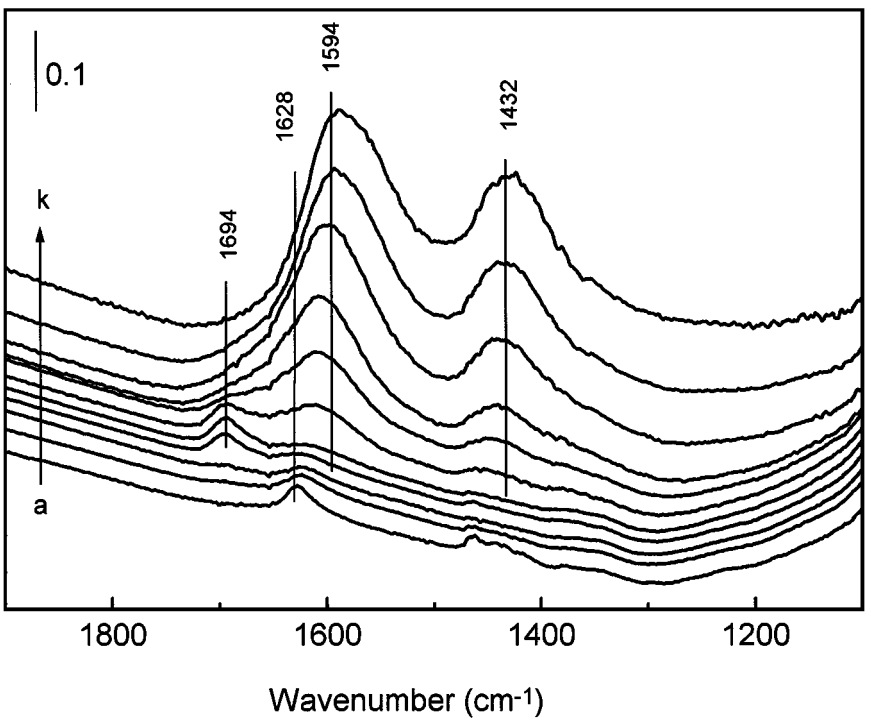

FIG. 3. FT-IR spectra of the VO_x/ESP catalyst outgassed at 500°C (a) and after adsorption of 1-butene at increasing temperatures: 25°C, 10 min (b); 100°C, 40 min (c); 150°C, 5 min (d); 150°C, 50 min (e); 200°C, 5 min (f); 200°C, 30 min (g); 250°C , 5 min (h); 250°C, 30 min (i); 350°C, 15 min (j); and 550°C, 30 min (k).

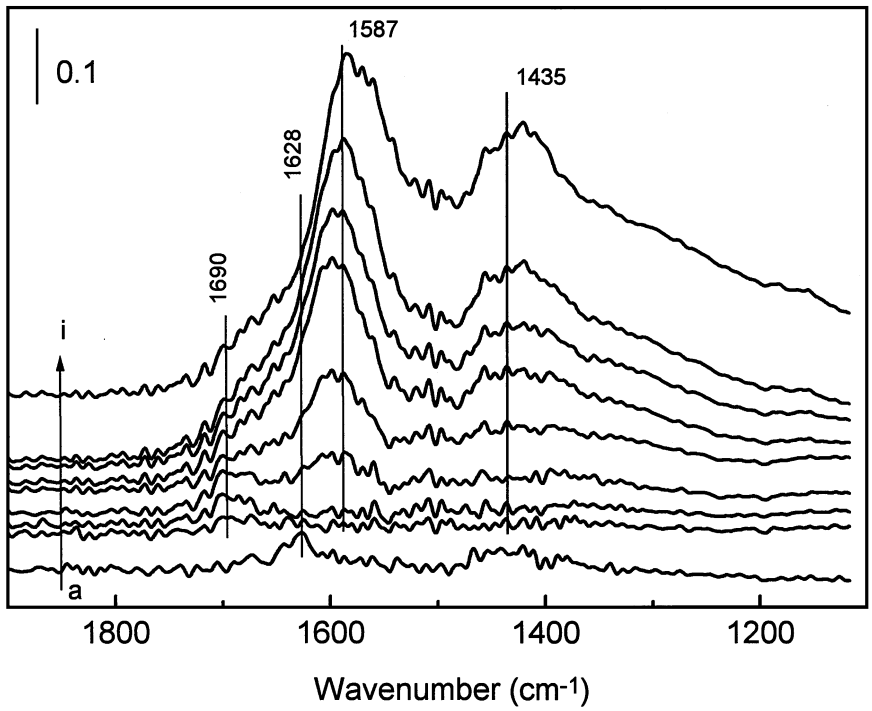

FIG. 4. FT-IR spectra of the VO_x/HT catalyst outgassed at 500°C (a) and after adsorption of 1-butene at increasing temperatures: 25°C, 50 min (b); 100°C, 30 min (c); 150°C, 5 min (d); 200°C, 60 min (e); 250°C, 5 min (f); 250°C, 60 min (g); 300°C, 60 min (h); and 350°C, 5 min (i).

band around 1694 cm^{-1} appears, assigned to some carbonyl species. These species are progressively oxidized by increasing the temperature from 200 to 400°C. Bands due to carboxylate species are observed at higher temperatures (broad strong bands at 1590 and 1432 cm^{-1}).

Figure 4 shows the spectra of the adsorbed species resulting from adsorption of 1-butene at room temperature on the VO_x/HT catalyst and their evolution at increasing temperatures. Due to the presence in the outgassed sample of strong bands at 1550 and 1350 cm^{-1} the identification of the adsorbed species resulting after interaction with 1-butene are studied by difference of these spectra with that of the clean sample. A similar behavior to that on VO_x/ESP is observed. At low temperature, molecularly adsorbed 1-butene species, which desorb by increasing the temperature, are formed. At higher temperatures, carbonyl species are observed which are oxidized to carboxylate compounds by progressively increasing of the temperature.

Oxidative Dehydrogenation of n-Butane

Table 1 shows the variation of the catalytic activity (in $mol_{C_4}\ h^{-1}\ g_{cat}^{-1}$) during the oxidative dehydrogenation of *n*-butane on supported vanadia catalysts. It can be seen that the catalytic activity for *n*-butane conversion increases in the following order: $VO_x/HT < VO_x/ESP = VMgO < VO_x/Al_2O_3$. A similar trend between the reducibility of V species on the catalysts and their catalytic activity can be observed in Table 1. Thus, it can be proposed that the catalyst reducibility could be involved in the rate-determining step (16, 17).

Figure 5a shows the selectivity to the OXDH products, i.e., 1-butene, *cis*-2-butene, *trans*-2-butene, and butadiene, with the *n*-butane conversion at 500°C on V-containing catalysts. No O-containing products other than CO and CO_2 were obtained. From the results of Fig. 5a it can be seen that the selectivity to OXDH products decreases as follows: $VMgO > VO_x/HT > VO_x/ESP > VO_x/Al_2O_3$, or, in other words, the absence of acid sites favors the OXDH of *n*-butane. However, not only the selectivity to C_4-olefins but the distribution of these olefins also depends on the catalyst nature. Thus, the data shown in Fig. 5b indicate that the 2-butene/(1-butene + butadiene) ratio decreases with the basic character of catalyst and that the formation of 1-butene and butadiene is favored by the presence of basic sites. This trend is in agreement with previously reported results in which the 1-butene/*cis*-2-butene/*trans*-2-butene molar ratio was close to an equilibrium ratio for acid catalysts (1 : 1 : 1.1) and close to a statistical ratio (3 : 1 : 1) for basic catalysts (17).

It has been suggested that the acid character of catalysts could modify the selectivity and distribution of olefins (5, 17). However, the distribution of final products may also be a consequence of the relative rates of secondary reactions. Thus, it should be informative to study the catalytic behavior of these catalysts in the oxydehydrogenation of both 1-butene and 2-butene.

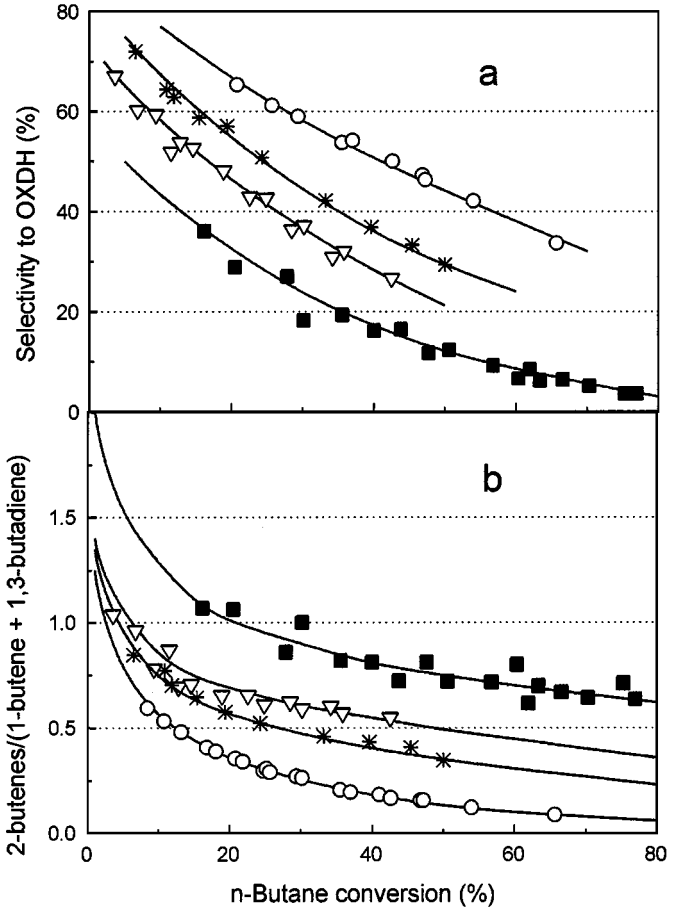

FIG. 5. Variation of the selectivity to OXDH products (a) and the 2-butenes/(1-butene + 1,3-butadiene) ratio with the *n*-butane conversion during the OXDH of *n*-butane on VMgO (○), VO_x/HT (✱), VO_x/ESP (▽), and VO_x/Al_2O_3 (■) at 500°C. Experimental conditions in text.

Oxidative Dehydrogenation of 1-Butene and trans-2-Butene

Table 2 summarizes the catalytic data obtained for supported vanadia catalysts during the oxidation of 1-butene. In all cases, butadiene, 2-butenes, and carbon oxides were the reaction products. However, while butadiene and carbon oxides are formed by oxidation reactions, i.e., oxydehydrogenation and deep oxidation, respectively, 2-butenes are formed by isomerization of 1-butene on acid sites (26, 35, 36).

Figure 6 shows the variation with the reaction temperature of both the isomerization/oxidation ratio, i.e., 2-butene/(butadiene + CO_x) (Fig. 6a), and the selectivity to butadiene defined as butadiene/(butadiene + CO_x) (Fig. 6b). The most acidic catalyst (VO_x/Al_2O_3) gives the higher isomerization/oxidation ratio at low temperature, and its selectivity to butadiene decreases with the reaction temperature. In contrast, the most basic catalyst (VMgO) develops a low isomerization/oxidation ratio and the selectivity to butadiene increases with the reaction temperature. VO_x/HT and VO_x/ESP catalysts show an intermediate catalytic behavior although their catalytic data are similar to those obtained for VMgO and VO_x/Al_2O_3, respectively. *Cis-*/*trans-* ratios near 1 and 1.1 were observed on basic (VMgO, VO_x/HT) and acid catalysts (VO_x/ESP and VO_x/Al_2O_3), respectively. The results of Fig. 6 suggest that the isomerization of 1-butene is an important competitive reaction, which is mainly catalyzed by acid sites at low temperatures.

Figure 7 shows the variation of the selectivity to butadiene with the conversion of 1-butene considering only oxidation products. As high butene conversions were obtained on VO_x/Al_2O_3 at relatively low contact times, the catalytic results obtained at 400°C have also been included. The selectivity to butadiene decreases in the following order: VMgO > VO_x/HT = VO_x/ESP > VO_x/Al_2O_3. This trend is similar to that obtained during the OXDH of *n*-butane and it appears that the absence of acid sites favors a higher selectivity to butadiene from 1-butene.

Table 3 shows the catalytic behavior of the acid (VO_x/Al_2O_3) and the basic (VMgO) catalysts during the oxidation of *trans*-2-butene. If we compare these results with those obtained with 1-butene (Table 2) it can be concluded

TABLE 2

Oxidative Dehydrogenation of 1-Butene on Supported Vanadium Oxide Catalysts

Catalyst	Temp. (°C)	W/F^a	Conversion (%)	Selectivity (%) 2-Butenes[b]	Butadiene[c]	CO_x[d]
VO_x/Al_2O_3	400	1.1	10.4	68.8	12.9	18.3
	450	1.1	22.9	53.4	13.3	33.3
	475	1.1	30.7	45.8	13.5	40.7
	500	1.1	39.4	37.1	13.2	49.7
	525	1.1	46.3	30.3	12.5	57.2
VO_x/ESP	400	10.1	13.5	38.4	22.0	39.6
	450	10.1	28.2	30.2	22.6	47.2
	475	10.1	37.1	26.1	23.0	50.9
	500	10.1	47.3	21.2	23.0	55.8
	525	10.1	57.9	16.4	21.7	61.9
VO_x/HT	400	10.1	3.7	22.1	20.5	57.4
	450	10.1	9.5	13.3	28.8	57.9
	475	10.0	14.6	11.5	33.0	55.5
	500	10.0	22.6	10.5	36.0	53.5
	525	10.0	30.8	9.0	37.7	53.3
VMgO	400	10.2	4.0	5.5	37.2	57.3
	450	10.2	10.6	3.1	44.6	52.3
	475	10.2	15.5	2.4	46.2	51.4
	500	10.2	24.7	2.0	49.4	48.6
	525	10.2	34.5	1.3	50.7	48.0

[a] W/F in g_{cat} h $(mol_{C_4})^{-1}$.
[b] Isomerization.
[c] Oxidative dehydrogenation.
[d] Deep oxidation.

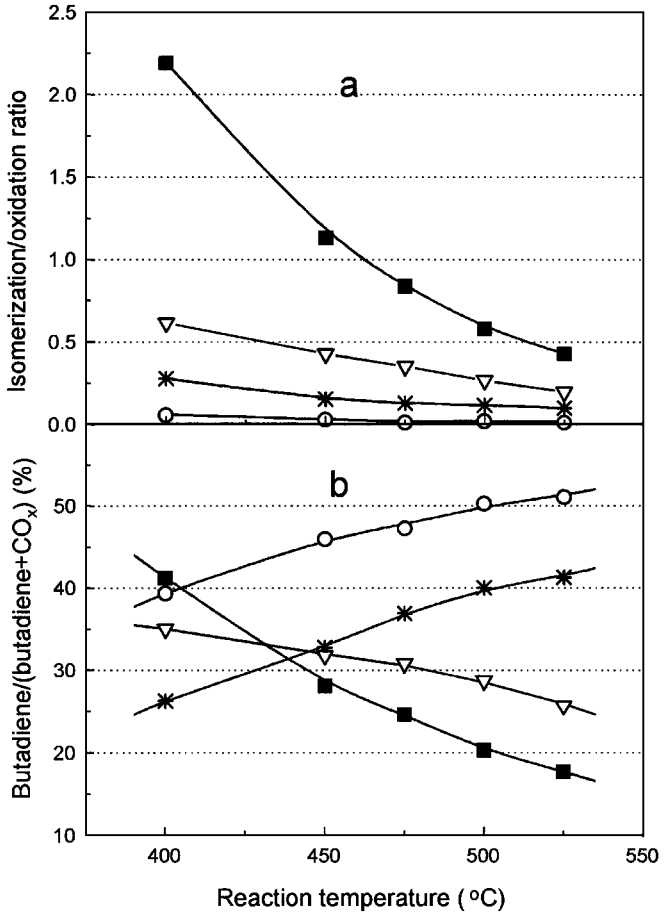

FIG. 6. Variation with the reaction temperature of the isomerization/oxidation ratio (a) and the selectivity to butadiene (b), expressed as the butadiene/(butadiene + CO_x) ratio, obtained during the OXDH of 1-butene on VMgO (○), VO_x/HT (✱), VO_x/ESP (▽), and VO_x/Al_2O_3 (■). Experimental conditions in Table 2.

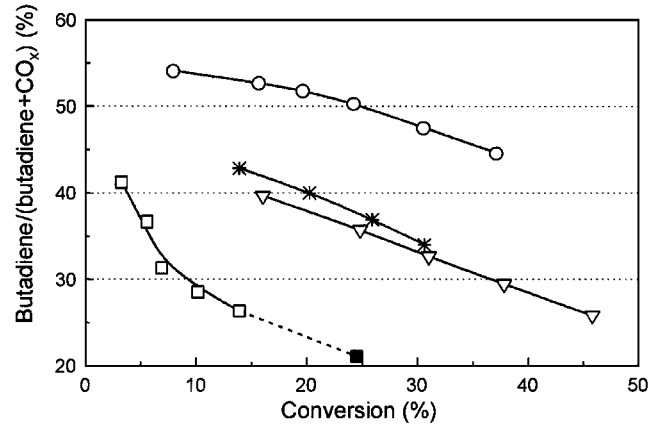

FIG. 7. Variation of the selectivity to butadiene with the 1-butene conversion during the OXDH of 1-butene at 500°C on VMgO (○), VO_x/HT (✱), VO_x/ESP (▽), and VO_x/Al_2O_3 (■) and at 400°C on VO_x/Al_2O_3 (□).

TABLE 3

Oxidative Dehydrogenation of *trans*-2-Butene on Supported Vanadium Oxide Catalysts

Catalyst	Temp. (°C)	W/F[a]	Conversion (%)	Selectivity (%) 1-Butene + c-2-butene[b]	Butadiene[c]	CO_x[d]
VO_x/Al_2O_3	400	1.1	9.2	46.7	25.6	27.7
	450	1.1	23.0	34.6	21.8	43.6
	475	1.1	33.4	30.4	19.4	50.2
	500	1.1	41.4	26.0	17.7	56.3
	525	1.1	50.8	20.8	16.2	63.0
VMgO	400	10.0	2.9	19.2	9.9	70.9
	450	10.0	9.2	4.2	29.0	66.8
	475	10.0	17.0	2.6	39.5	57.9
	500	10.0	30.2	1.4	49.2	49.4
	525	10.0	42.6	1.2	55.9	42.9

[a] W/F in g_{cat} h $(mol_{C_4})^{-1}$.
[b] Isomerization.
[c] Oxidative dehydrogenation.
[d] Deep oxidation.

that both olefins present similar reactivities. Both isomerization and oxidation reactions occur with *trans*-2-butene as has been observed with 1-butene. Thus, 1-butene and *cis*-2-butene (formed by the isomerization reaction), butadiene (formed by oxydehydrogenation), and carbon oxides (deep oxidation) are the main reaction products during the oxidation of *trans*-2-butene. We must indicate that a 1-butene/*cis*-2-butene ratio near to 1 was observed in all cases although the selectivity to reaction products also depends on the catalyst studied.

Figure 8 shows the variation of both the isomerization/oxidation ratio, i.e., 2-butene/(butadiene + CO_x) (Fig. 8a), and the selectivity to butadiene expressed as butadiene/(butadiene + CO_x) (Fig. 8b) with the reaction temperature. As discussed above for the oxidation of 1-butene, the isomerization of *trans*-2-butene to 1-butene and *cis*-2-butene (at low temperature) and the formation of carbon oxides (at high temperatures) are mainly observed on the acid catalyst (VO_x/Al_2O_3). The VMgO catalyst is selective in the oxidation of monoolefins to butadiene.

It must be emphasized that a similar trend in the selectivity to butadiene was achieved from both 1-butene (Fig. 6b) and *trans*-2-butene (Fig. 8b). Thus, it appears that the distribution of reaction products obtained from *n*-butane on the studied catalysts does not depend on the nature of primary products formed from *n*-butane, i.e., 1-butene or 2-butene, but on the reaction rate of consecutive reactions as it has been suggested previously. Thus, the isomerization reaction at low reaction temperature and deep oxidation at high reaction temperature are favored on acid catalysts while basic catalysts favor the oxydehydrogenation reactions.

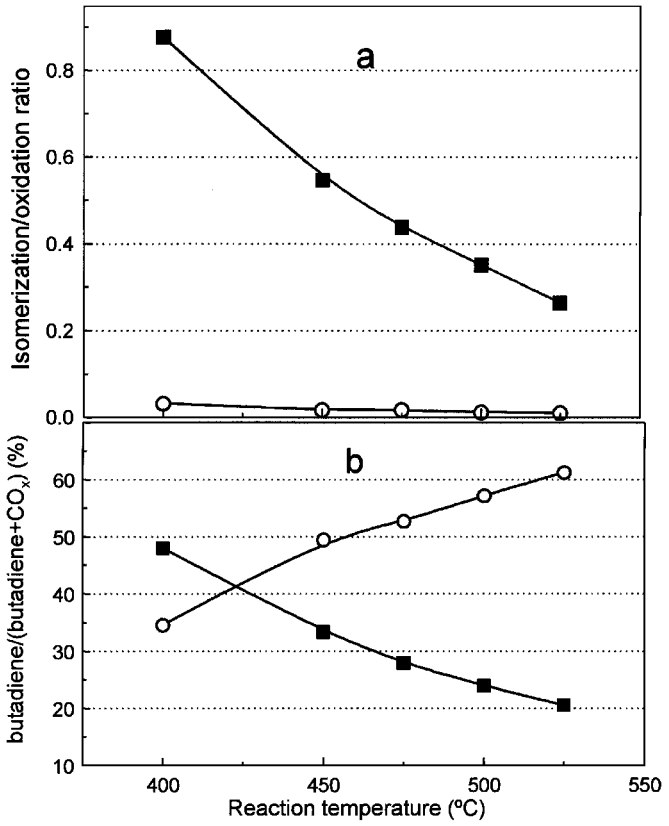

FIG. 8. Variation with the reaction temperature of the isomerization/oxidation ratio (a) and the selectivity to butadiene (b), expressed as the butadiene/(butadiene + CO_x) ratio, obtained during the OXDH of *trans*-2-butene on VMgO (○) and VO_x/Al_2O_3 (■). Experimental conditions in Table 3.

MECHANISTIC CONSIDERATIONS

From the catalytic results obtained during the oxidation of *n*-butane and butenes on supported vanadium oxide catalysts, the reaction network shown in Scheme 1 is proposed for the transformation of *n*-butane and butenes. According to a previously suggested mechanism for the *n*-butane oxidation (5–7), the reaction can be initiated by hydrogen abstraction forming a butyl species. A second H abstraction is needed to obtain intermediate monoolefins which may subsequently be desorbed forming the corresponding olefins. These olefins preferentially isomerize at low temperature or form carbon oxides at high temperatures on acid catalysts. The IR results reported in this paper indicate the presence of carbonyl and alkoxide species formed by the interaction of the olefin with the acid sites of alumina.

In the case of supported vanadia catalysts with a basic character monoolefins can be readsorbed and butadiene is formed by an allylic mechanism, in a consecutive step. In the present paper, we observed the formation of butadiene from 1-butene (Fig. 2). Acetone or bicarbonate species are also observed on these catalysts as minority species, which may be formed via interaction of olefins with the free MgO support. However, carbonyl and alkoxide species as observed on VO_x/Al_2O_3 were not observed on the MgO-based materials.

Recently, Ramani *et al.* studied the isomerization (26) and the oxidation (37) of 1-butene on supported metal oxides. They concluded that, while on Cr-containing catalysts the isomerization of 1-butene to 2-butene proceeds via an allylic mechanism, on Mo- or W-containing catalysts the isomerization could be carried out by Brønsted acid sites (low temperatures) or by an oxidative dehydrogenation pathway (high reaction temperatures). The different mechanism on Cr-based catalysts was explained on the basis of its high reducibility. Therefore, the redox ability of the supported catalysts was inferred to have a prominent influence on the selective oxidation of 1-butene.

The present results suggest that an allylic mechanism could operate in the case of VO_x/Al_2O_3 catalysts at low temperatures, since it presents the highest reducibility among the investigated materials. However, when acid sites are present the isomerization of olefins can be faster and may become the dominant mechanism on the catalyst surface. In fact, if we compare the catalytic behavior of samples with different reducibility but with similar acid character, namely VO_x/Al_2O_3 and VO_x/ESP, it can be seen that

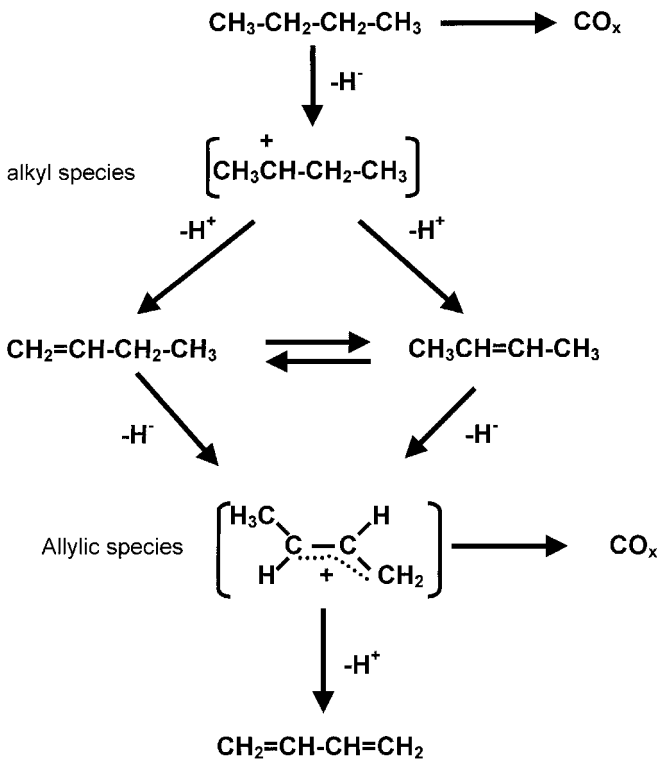

SCHEME 1. Reation network for the OXDH of *n*-butane and butenes on supported vanadium oxide catalysts.

both catalysts show similar olefin/diolefin ratios. This catalytic performance is similar to that observed on molybdate-based catalysts in which the presence of acid sites favors the isomerization at low temperature and the deep oxidation at high temperature, while the absence of acid sites favors the selective formation of butadiene (35, 36). We must indicate that the catalytic behavior of VO_x/Al_2O_3 catalyst is strongly modified after the incorporation of potassium in the same way than that observed here (13): the higher the K-loading the lower the number of lewis acid sites and the higher the selectivity to OXDH products from *n*-butane. Thus, it appears that for these catalysts the reaction rate for the isomerization on acid sites is more faster than the isomerization of butenes by an allylic mechanism.

In contrast, the allylic mechanism must preferentially operate on catalysts with basic character, especially at the high reaction temperatures employed in this work. In this case, butadiene will be selectively formed.

These results are also in agreement with the mechanism proposed by Busca *et al.* for the oxydehydrogenation of *n*-butane and butenes from the IR results obtained for the interaction of several molecules, such as alkanes, olefins, and alcohols, on selective (Mg-vanadates) and nonselective (ferrites) catalysts (21, 24). The authors observed a very low reactivity of Mg-vanadates for forming the alkoxide species which are rapidly decomposed while on nonselective catalysts the alkoxide species are rapidly formed and transformed to carbon oxides.

The redox properties of catalysts could influence their catalytic behavior for formation of both the butyl radical during the activation of *n*-butane and the formation of an allylic intermediate during the activation of olefins. In these cases the catalyst reducibility appears to be the rate-determining step, especially at low reaction temperature (38–40). However, the acid–base character of the catalyst determines the selectivity toward oxydehydrogenation products.

It has been observed that supported vanadium oxide catalysts present similar initial selectivities to OXDH products (at low conversion of *n*-butane) but they strongly decrease with the acid character of catalysts at high butane conversions. At low butane conversions, Me sites vanadium free on the surface of the active matrix, i.e., MgO (5), Al_2O_3 (15), SiO_2 (41), and $AlPO_4$ (42), are responsible for the formation of CO_x from *n*-butane. However, the different selectivity to OXDH products observed at high butane conversions can be explained by the different interaction between the olefinic intermediates and the catalyst which can be determined by the presence of acid and/or basic sites as suggested by Dadyburjor *et al.* (1). In this case the formation of CO_x from olefins will depend on the residence time of intermediates on the catalyst surface.

Thus, and according to our results, the second H abstraction and/or the desorption of olefinic intermediates appears to be the selectivity-determining step. In both cases, basic catalysts will present better selectivities to olefins than the corresponding acid catalysts since they will favor a fast desorption of olefinic intermediates, thus decreasing the consecutive reactions.

CONCLUSION

From the catalytic results obtained during the oxidation of *n*-butane and butenes on supported vanadium oxide catalysts it can be concluded that both the acid–base character and the redox ability of the catalysts determine their catalytic behavior.

The presence of acid sites favors slow desorption of olefinic intermediates and their isomerization prior to desorption. As a consequence of this performance, 2-butene is mainly formed at low reaction temperatures while the deep oxidation is observed at high reaction temperatures. In this case, infrared results of 1-butene adsorbed on VO_x/Al_2O_3 indicate the interaction of 1-butene with acid sites forming O-containing adsorbed species, namely carbonyl and alkoxide species, which are the precursors for the formation of carboxylates and carbonates and finally carbon oxides.

Basic catalysts, in contrast, favor a fast desorption of olefinic intermediates (17) and both olefins and diolefins are selectively formed from *n*-butane or butenes. Our infrared results of 1-butene adsorbed on basic catalysts show the presence of adsorbed butadiene species. Carbon oxides might be formed in a parallel reaction with the formation of acetone on V-free sites of the support at low temperature. However, oxygen-containing species, such as alkoxide and carbonyl species, were not observed on basic materials.

In the case of catalysts supported on Mg–Al–O mixed oxides, with an acid–base character intermediate between Al_2O_3 and MgO, the catalytic behavior depends on the Mg/Al ratio. Catalysts with high Al content present a catalytic behavior similar to that of the VO_x/Al_2O_3 catalyst, while catalysts with high Mg content show a catalytic behavior similar to that of VMgO catalyst.

ACKNOWLEDGMENTS

The Spanish authors thank the financial contribution by Comisión Interministerial de Ciencia y Tecnología, CICYT, from Spain (Project MAT 97-0561). The work done in München was financially supported by the Deutsche Forschungsgemeinschaft (SFB 338) and by the Fonds der Chemischen Industrie. P.C. acknowledges a grant from the Fonds der Chemischen Industrie.

REFERENCES

1. Dadyburjor, D. B., Jewur, S. S., and Ruckenstein, E., *Catal. Rev. Sci. Eng.* **19**, 293 (1979).
2. Bond, G. C., and Tahir, S. F., *Appl. Catal.* **71**, 1 (1991).
3. Vedrine, J. C., *Stud. Surf. Sci. Catal.* **110**, 61 (1997).
4. Albonetti, S., Cavani, F., and Trifiró, F., *Catal. Rev. Sci. Eng.* **38**, 413 (1996).

5. Blasco, T., and López Nieto, J. M., *Appl. Catal. A* **157**, 117 (1997).
6. Kung, H. H., Kung, M. C., *Appl. Catal. A* **157**, 105 (1997).
7. Chaar, M. A., Patel, D., Kung, M. C., and Kung, H. H., *J. Catal.* **105**, 483 (1987).
8. Sam, D. S. H., Soenen, V., and Volta, J. C., *J. Catal.* **123**, 417 (1990).
9. Corma, A., López Nieto, J. M., and Paredes, N., *J. Catal.* **144**, 425 (1993).
10. Gao, X., Ruíz, P., Xin, Q., Guo, X., and Delmon, B., *J. Catal.* **148**, 56 (1994).
11. Pantazidis, A., Aurous, A., Hermann, J.-M., and Mirodatos, C., *Catal. Today* **32**, 81 (1996).
12. Le Bars, J., Auroux, A., Forissier, M., and Vedrine, J. C., *J. Catal.* **162**, 250 (1996).
13. Galli, A., López Nieto, J. M., Dejoz, A., and Vázquez, M. I., *Catal. Lett.* **34**, 51 (1995).
14. Cavani, F., and Trifiró, F., *Catal. Today* **24**, 307 (1995).
15. Blasco, T., Galli, A., López Nieto, J. M., and Trifiró, F., *J. Catal.* **169**, 203 (1997).
16. Concepción, P., Galli, A., López Nieto, J. M., Dejoz, A., and Vázquez, M. I., *Topic Catal.* **3**, 451 (1996).
17. Blasco, T., Dejoz, A., López Nieto, J. M., and Vázquez, M. I., *J. Catal.* **157**, 271 (1995).
18. Deo, G., and Wachs, I. E., *J. Phys. Chem*. **95**, 5889 (1991).
19. Deo, G., Wachs, I. E., and Haber, J., *Crit. Rev. Surf. Chem*. **4**, 141 (1994).
20. Vedrine, J. C., Millet, J. M. M., and Volta, J. C., *Catal. Today* **32**, 115 (1996).
21. Busca, G., Finocchio, E., Ramis, G., and Ricchiardi, G., *Catal. Today* **32**, 133 (1996)
22. Blasco, T., and López Nieto, J. M., *Colloid Surf. A* **115**, 187 (1996).
23. Busca, G., *Catal. Today* **27**, 457 (1996).
24. Trombetta, M., Busca, G., Rossini, S. A., Piccoli, V., and Cornaro, U., *J. Catal.* **168**, 334 (1997).
25. Escribano, V. S., Busca, G., and Lorenzelli, V., *J. Phys. Chem*. **95**, 5541 (1991).
26. Ramani, N. C., Sullivan D. L., and Ekerdt, J. G., *J. Catal.* **173**, 105 (1998).
27. Chang, C. C., Conner, W. C., and Kokes, R. J., *J. Phys. Chem*. **77**, 1957 (1973).
28. Dent, A. L., and Kokes, R. J., *J. Phys. Chem*. **75**, 487 (1971).
29. Busca, G., Ramis, G., Lorenzelli, V., Janin, A., and Lavalley, J. C., *Spectrochim. Acta A* **43**, 489 (1987).
30. Knözinger, H., Krietenbrink, H., Müller, H. D., and Schulz, W., "Proceedings, 6th International Congress on Catalysis, London 1976" (G. C. Bond, P. B. Wells, and F. C. Tompking, Eds.), Vol. 1, p. 183. The Chemical Society, London, 1977.
31. Lin-Vien, D., Colthup, N. B., Fateley, W. G., and Grasselli, J. G., "The Handbook of Infrared and Raman Characteristic Frequencies of Organic Molecules." Academic Press, San Diego, 1991.
32. Busca, G., and Lorenzelli, V., *Mater. Chem*. **5**, 213 (1980).
33. Escribano, V. S., Busca, G., and Lorenzelli, V., *J. Phys. Chem*. **94**, 8939 (1990).
34. Busca, G., Ramis, G., and Lorenzelli, V., *J. Mol. Catal.* **55**, 1 (1989).
35. Mori, K., Inomata, M., Miyamoto, A., and Murakami, Y., *J. Phys. Chem*. **87**, 4560 (1983).
36. Forzatti, P., Trifiró, F., and Villa, P. L., *J. Catal.* **52**, 389 (1978).
37. Ramani, N. C., Sullivan, D. L., Ekerdt, J. G., Jehng, J.-M., and Wachs, I. E., *J. Catal.* **176**, 143 (1998).
38. Soler, J., López Nieto, J. M., Herguido, J., Menéndez, M., and Santamaría, J., *Catal. Lett.* **50**, 25 (1998).
39. López Nieto, J. M., Dejoz, A., Vázquez, M. I., O'Leary, W., and Cunningham, J., *Catal. Today* **40**, 215 (1998).
40. López Nieto, J. M., Soler, J., Concepción P., Herguido, J., Menéndez, M., and Santamaría, J., *J. Catal.* **185**, 324 (1999).
41. Le Bars, J., Vedrine, J. C., Auroux, A., Trautmant, S., and Baerns, M., *Appl. Catal. A* **88**, 179 (1992).
42. Andersson, S. L. T., *Appl. Catal. A* **112**, 209 (1994).